Surface Science 122 (1982) 459–473
North-Holland Publishing Company

DIFFUSION ON SURFACES OF FINITE SIZE: MÖSSBAUER EFFECT AS A PROBE

Peter S. RISEBOROUGH and Peter HANGGI

Department of Physics, Polytechnic Institute of New York, 333 Jay Street, Brooklyn, New York, 11201, USA

Received 22 June 1982; accepted for publication 1 September 1982

In this manuscript, we present a theoretical analysis of the Mössbauer spectrum of a particle diffusing on surfaces of finite size. The spectrum exhibits a broadening of the linewidth, which has a characteristic size dependence associated with it. We present explicit results for spherical surfaces and discs with various types of boundary conditions. The spectrum is sensitive to the type of boundary condition. The Mössbauer spectrum can be used as an independent technique for surface diffusion studies, and can be compared with the results obtained from field ion microscopy investigations. Field ion microscopy studies focus on the mean squared displacement of the particles. Using the same formalism, we present results for the mean squared displacement of particles on small domains subject to varying boundary conditions.

1. Introduction

Diffusion of atoms on a surface of a solid has long been the subject of scientific interest [1,2]. It has an important role in many technologicl processes, such as crystal and thin film growth, the formation of epitaxial layers, surface oxidization, heterogeneous catalysis, etc. However, very few good probes of the rate of diffusion of the adsorbed atoms exist. Field ion microscopy [3] is a technique that allows one to investigate diffusion on smooth surfaces. In such studies successive images are formed of adsorbed atoms on surfaces that are typically smaller than 100 Å in diameter. From a knowledge of the displacement $\boldsymbol{r}(t)-\boldsymbol{r}(0)$ of the atom and the time elapse between successive imagings one can deduce a diffusion coefficient D. Field ion microscopy studies have shown that single adatoms on the (111) and (100) planes of rhodium and the (110) plane of tungsten can be described by simple diffusion.

Despite these successful results there are some experimental difficulties associated with the technique. The first is that of measuring the absolute distances between the position of the adatoms [2]. Only surfaces with lattice spacings of at least 3 Å can be resolved directly. The second difficulty is associted with the size of the surface used in field ion microscopy. Since the surfaces are less than 100 Å in diameter [1,2], the motion of an adatom wil be strongly effected by the surface after only a few jumps. The adatoms may be preferentially bound by either the interior of the plane or the edge of the plane. This will strongly effect the result for the mean square displacement, for example if one assumes reflecting boundaries one obtains

$$\langle (\boldsymbol{r}(t)-\boldsymbol{r}(0))^2 \rangle = 4a^2 \left(\frac{1}{4} - 2 \sum_{n=1}^{\infty} \frac{\exp(-\beta_n^2 Dt/a^2)}{\beta_n^2(\beta_n^2-1)} \right),$$

where β_n are the solutions of

$$\frac{\partial}{\partial z} J_1(z) = 0,$$

In which $J_1(z)$ is the Bessel function of order 1. Clearly, a clever deconvolution of the diffusion coefficient and the boundary conditions must be made. Another experimental probe of the motion could be extremely useful, to aid such a deconvolution.

In this paper, Mössbauer measurements [4,5] are proposed to provide independent information on the diffusion coefficients of atoms on single surfaces as well as on the size and boundaries of the surface. Alternatively, the Mössbauer effect could be used in the study of surface migration of ligands to active sites on sphere like proteins or enzymes [6,7], or energy transfer [8].

The experiment that we propose, consists of Mössbauer atoms absorbed, in dilute concentrations, on small surfaces. These atoms, which we assume to diffuse, act as a source for γ-rays. The detector would consist of a bulk slab containing a high concentration of Mössbauer atoms which are assumed to have negligible diffusion. The resulting signal is then expected to have a shape that is characteristic of an atom diffusing on a surface of finite area. The spectrum is expected to be composed of an unbroadened quasi-elastic peak superimposed on a broad background. The strength of the quasi-elastic peak and the width of the wings is expected to be determined by the size of the surface area, the nature of the perimeter of the surface and the diffusion coefficient. As a specific example, we consider a surface that has islands or terraces which have sizes in the range of tens to hundreds of ångströms. A finite concentration of Mössbauer atoms on such a surface should give a signal intensity strong enough to be observed. At helium temperatures, the signal is expected to be in the form of the natural spectrum as the diffusion processes are usually thermally activated [1]. As the temperature increases we expect that the line will be broadened due to the diffusion and that the unbroadened component can be used to provide an estimate of the characteristic size of the islands or terraces.

In section 2, we shall discuss the Mössbauer spectrum of particles diffusing on surfaces of finite size; first on spheres and then on discs.

2. The Mössbauer cross-section

We shall assume that our Mössbauer atoms are sufficiently dilute that the diffusion is unaffected by the presence of other atoms. The atoms are free to diffuse over the surface. The probability $P(\boldsymbol{r}, \boldsymbol{r}_0|t)$ that an atom, initially at $\boldsymbol{r}_0$ ($t = 0$), is at position $\boldsymbol{r}$ at time t is governed by the diffusion equation

$$\frac{\partial P}{\partial t}(\boldsymbol{r}, \boldsymbol{r}_0|t) = D\,\nabla_r^2 P(\boldsymbol{r}, \boldsymbol{r}_0|t), \tag{2.1}$$

together with the constraint that the particle lies on the surface [10]. If the initial distribution of atoms is given by $p(\boldsymbol{r}_0)$, the Mössbauer cross-section [9] is given by

$$I(\omega, \boldsymbol{q}) = \int_0^\infty \frac{\mathrm{d}t}{\pi} \exp(-\Gamma t/2) \cos \omega t \int \mathrm{d}\boldsymbol{r}_0\, p(\boldsymbol{r}_0) \int \mathrm{d}\boldsymbol{r}\, P(\boldsymbol{r}, \boldsymbol{r}_0|t) \times \exp[\mathrm{i}\boldsymbol{q}(\boldsymbol{r} - \boldsymbol{r}_0)], \tag{2.2}$$

in which q is the γ-ray momentum, and $\Gamma/2$ the natural linewidth. (For Fe^{57}: $q = 7.27 \times 10^{10}\ \mathrm{m}^{-1}$ and $\Gamma = 0.71 \times 10^7\ \mathrm{s}^{-1}$.)

We shall, for simplicity, first consider the motion to be confined to the surface of a sphere of radius a. It is most convenient to transform to polar coordinates $\boldsymbol{r} = (a, \theta, \psi)$. The solution for the probability $P(\boldsymbol{r}, \boldsymbol{r}_0|t)$ is then found by expanding in terms of the spherical harmonics,

$$P(\boldsymbol{r}, \boldsymbol{r}_0|t) = \sum_{l=0}^{\infty} \sum_{m=-l}^{l} A_l^m(\theta_0, \psi_0|t)\, Y_l^m(\theta, \psi). \tag{2.3}$$

On using the orthonomality properties of $Y_l^m(\theta, \psi)$ we find that the coefficients $A_l^m(\theta_0, \psi_0|t)$ satisfy the equation

$$\frac{\partial}{\partial t} A_l^m(\theta_0, \psi_0|t) = -\frac{Dl(l+1)}{a^2} A_l^m(\theta_0, \psi_0|t). \tag{2.4}$$

Solving this equation and then using the completeness relations to specify the initial amplitudes $A_l^m(\theta_0, \psi_0|0)$ we find the solution

$$P(\boldsymbol{r}, \boldsymbol{r}_0|t) = \sum_{l=0}^{\infty} \sum_{m=-l}^{l} Y_l^m(\theta, \psi)\, Y^{*m}_l(\theta_0, \psi_0) \exp\left(\frac{-Dl(l+1)\,t}{a^2}\right). \tag{2.5}$$

We shall define the polar axis to be in the direction of the emitted γ-ray. Thus we have

$$\boldsymbol{q}(\boldsymbol{r}(t) - \boldsymbol{r}(0)) = qa(\cos\theta(t) - \cos\theta(0)). \tag{2.6}$$

Substituting this in eq. (2.2) and utilizing the expansion of a plane wave in terms of spherical Bessel functions,

$$\exp(\mathrm{i}qa\cos\theta) = \sum_{l=0}^{\infty} (2l+1)\, j_l(qa)\, \mathrm{i}^{-l} P_l(\cos\theta), \tag{2.7}$$

we find that for a uniform initial distribution $p(\boldsymbol{r}_0) = 1/4\pi$ the spectrum is given by

$$I(\omega, q) = \frac{1}{\pi} \sum_{l=0}^{\infty} (2l+1)\, j_l^2(qa) \frac{Dl(l+1)/a^2 + \Gamma/2}{\omega^2 + \left[Dl(l+1)/a^2 + \Gamma/2\right]^2}. \tag{2.8}$$

Thus the Mössbauer spectrum for particles diffusing on the surface of a sphere consists of a superposition of Lorentzians of weight $(2l+1) j_l^2(qa)$, centered at $\omega = 0$, each with width $Dl(l+1)/a^2 + \Gamma/2$. The total integrated strength remaining a constant. Note that the spectrum contains a sharp inelastic line, $l = 0$, with weight $\sin^2 qa/q^2a^2$.

The size dependence occurs in the weights of the Lorentzians only, i.e. via the dimensionless parameter qa. In the limit of vanishing size ($aq \to 0$) we recover the Mössbauer spectrum corresponding to a single particle unable to diffuse,

$$\lim_{qa \to 0} I(\omega, q) = \frac{1}{\pi} \frac{\Gamma/2}{\omega^2 + (\Gamma/2)^2}.$$

On increasing the size of the sphere the overall linewidth of the spectrum increases, the higher angular momentum eigenstates becoming increasingly important. Contributions from angular momentum eigenstates such that

$$l(l+1) > q^2a^2$$

are negligible. For the size of the sphere approaching infinity, we recover the spectrum for an infinite plane

$$\lim_{qa \to \infty} I(\omega, q) = \frac{1}{\pi} \frac{Dq^2 + \Gamma/2}{\omega^2 + (Dq^2 + \Gamma/2)^2}.$$

In figs. 1a and 1b we have plotted the Mössbauer spectrum calculated for two different values of the diffusion coefficient. In these calculations we have used $qa \simeq 180$ which corresponds to a radius of roughly 25 Å for Fe^{57}. In fig. 1a, $\Gamma a^2/2D = 0.2$, i.e. $D = 10^{-10}$ m^2 s^{-1}, and in fig. 1b, $\Gamma a^2/2D = 2000$. Fig. 1a corresponds roughly to the diffusion of O on W(110) at temperatures of 1200 K. In the spectrum one can clearly observe the unbroadened quasi-elastic contribution, which has intensity proportional to a^{-2}.

We shall now investigate the Mössbauer spectrum expected for an atom diffusing on a disc of radius a, in order to make direct comparison with the field ion microscopy data. The boundary conditions we use are

$$P(\boldsymbol{r}, \boldsymbol{r}_0|t) + \kappa \boldsymbol{r} \cdot \nabla \boldsymbol{r} P(\boldsymbol{r}, \boldsymbol{r}_0|t)_{|\boldsymbol{r}|=a} = 0. \tag{2.9}$$

These conditions include the special limits of completely reflecting ($\kappa \to \infty$) and absorbing perimeter ($\kappa \to 0$). The condition probability $P(\boldsymbol{r}, \boldsymbol{r}_0|t)$ for a particle remaining inside the boundary is given by (see appendix A)

$$P(\boldsymbol{r}, \boldsymbol{r}_0|t) = \frac{1}{\pi a^2} \sum_{m=-\infty}^{\infty} \sum_{n=1}^{\infty} \exp[-im(\psi - \psi_0)]$$
$$\times \frac{\kappa^2 \beta_{mn}^2 J_m(\beta_{mn} r/a) J_m(\beta_{mn} r_0/a)}{[1 + \kappa^2(\beta_{mn}^2 - m^2)] J_m^2(\beta_{mn})} \exp(-D\beta_{mn}^2 t/a^2), \qquad (2.10)$$

where the β_{mn} are the solutions of

$J_m(z) + \kappa z J_m'(z) = 0.$

The probability $Q(\boldsymbol{r}, \boldsymbol{r}_0|t)$ that a particle initially at $\boldsymbol{r}_0$, ends up absorbed on the boundary at $\boldsymbol{r}$, up to time t, is given by

$$Q(\boldsymbol{r}, \boldsymbol{r}_0|t) = \frac{1}{\pi} \sum_{m=-\infty}^{\infty} \sum_{n=1}^{\infty} \exp[-im(\psi - \psi_0)]$$
$$\times \kappa \frac{J_m(\beta_{mn} r_0/a)}{J_m(\beta_{mn})} \frac{1 - \exp(-D\beta_{mn}^2 t/a^2)}{1 + \kappa^2(\beta_{mn}^2 - m^2)}, \quad |\boldsymbol{r}| = a. \qquad (2.11)$$

We note that as the boundary becomes purely reflecting ($\kappa \to \infty$) the probability of absorption Q vanishes. In the opposite limit of completely absorbing boundaries ($\kappa \to 0$), Q remains finite since $J_m(\beta_{mn})$ also vanishes.

The Mössbauer spectrum is calculated, in appendix A, as

$$I(\omega, q) = \frac{4}{\pi} \sum_{m=-\infty}^{\infty} \sum_{n=1}^{\infty} \frac{J_m(q_\parallel a) + \kappa q_\parallel a J_m'(q_\parallel a)}{(\beta_{mn}^2 - q_\parallel^2 a^2)[1 + \kappa^2(\beta_{mn}^2 - m^2)]}$$
$$\times \left\{ \frac{J_m(q_\parallel a)\, q_\parallel^2 a^2 + \beta_{mn}^2 \kappa q_\parallel a J_m(q_\parallel a)}{\beta_{mn}^2 - q_\parallel^2 a^2} \frac{D\beta_{mn}^2/a^2 + \Gamma/2}{\omega^2 + (D\beta_{mn}^2/a^2 + \Gamma/2)^2} \right.$$
$$\left. + J_m(q_\parallel a) \frac{\Gamma/2}{\omega^2 + (\Gamma/2)^2} \right\}, \qquad (2.12)$$

in which we have used a uniform initial distribution and $q_\parallel$ is the component of the γ-ray momentum parallel to the surface.

In (2.12) there are two contributions, one from the particles which remain within the perimeter of the disc, and a second contribution from the particles absorbed on the boundary. The last term in the curly brackets represents the time independent part of the spectrum from the absorbed particles. Since these are stationary, the contribution is unbroadened and has only the natural Mössbauer line width $\Gamma/2$.

In general, it is the finite size of the system that allows for a finite stationary probability distribution of the particles, in the asymptotic long-time limit. It is this fact that leads to an unbroadened quasi-elastic contribution to the Mössbauer spectrum.

The field ion microscopy studies have focused on the mean squared displacement $\sigma(t)$ of the diffusing particle. This quantity also depends on the boundary conditions. We shall calculate $\sigma(t)$ in appendix B,

$$\sigma(t) = \langle (\boldsymbol{r}(t) - \boldsymbol{r}(0))^2 \rangle, \tag{2.13}$$

for comparison with the Mössbauer formula (2.12);

$$\sigma(t) = 8a^2 \left\{ \sum_{n=1}^{\infty} \frac{\left[\beta_{0n}^2(1+\kappa) - 2\right] + \left(\kappa\beta_{0n}^2 - 2\right)\exp\left(-D\beta_{0n}^2 t/a^2\right)}{\beta_{0n}^4\left(1+\kappa^2\beta_{0n}^2\right)} - \sum_{n=1}^{\infty} \frac{(\kappa+1) + \kappa(\kappa+1)\exp\left(-D\beta_{1n}^2 t/a^2\right)}{\beta_{1n}^2\left[1+\kappa^2\left(\beta_{1n}^2 - 1\right)\right]} \right\}. \tag{2.14}$$

In the limit of reflecting boundaries, $\kappa \to \infty$,

$$\sigma(t) = 4a^2 \left\{ \frac{1}{4} - \sum_{n=1}^{\infty} \frac{2}{\beta_{1n}^2\left(\beta_{1n}^2 - 1\right)} \exp\left(-D\beta_{1n}^2 t/a^2\right) \right\}, \tag{2.15}$$

a

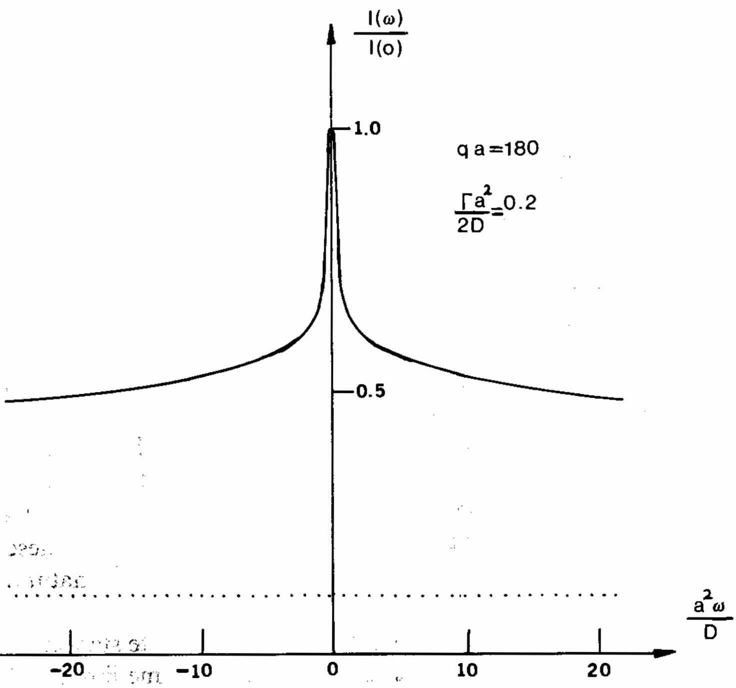

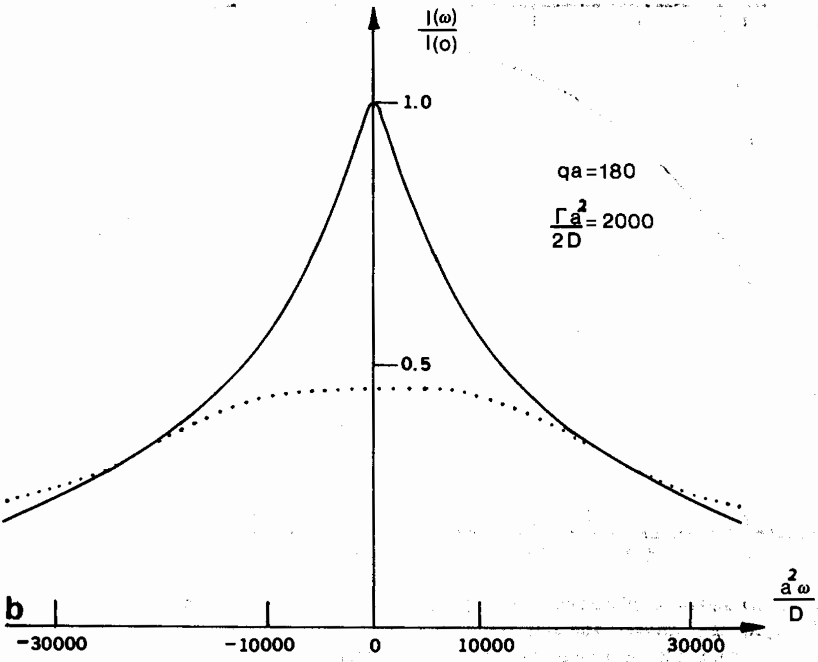

Fig. 1. (a) The Mössbauer spectrum for a particle diffusing on a sphere, plotted in dimensionless units. A separation between the quasi-elastic and inelastic part is possible (Fe^{57}, $D = 10^{-10}$ m^2 s^{-1}, $a = 25$ Å). The dotted line corresponds to the result expected from an infinite plane. (b) The Mössbauer spectrum for diffusion on the surface of a sphere (Fe^{57}, $D = 10^{-14}$ m^2 s^{-1}, $a = 25$ Å). The dotted line corresponds to the infinite plane limit $qa \to \infty$.

where

$$J_1'(\beta_{1n}) = 0.$$

This result is plotted in fig. 2 as a function of the dimensionless quantity $\tau = Dt/a^2$ and $y(\tau) = \sigma(t)/a^2$. In contrast to the result for the infinite plane, the mean square displacement is bounded by a^2 in the limit $t \to \infty$. For short times $t \to 0$, $\sigma(t)$ vanishes, since

$$\sum_{n=1}^{\infty} \frac{2}{\beta_{1n}^2(\beta_{1n}^2 - 1)} = \frac{1}{4},$$

as shown in appendix C. The initial slope, however, yields the infinite plane result

$$\lim_{t \to 0} \frac{\partial \sigma(t)}{\partial t} = \lim_{t \to 0} 4D \sum_{n=1}^{\infty} \frac{2}{\beta_{1n}^2 - 1} \exp\left(-D\beta_{1n}^2 t/a^2\right) = 4D, \tag{2.16}$$

as also shown in appendix C.

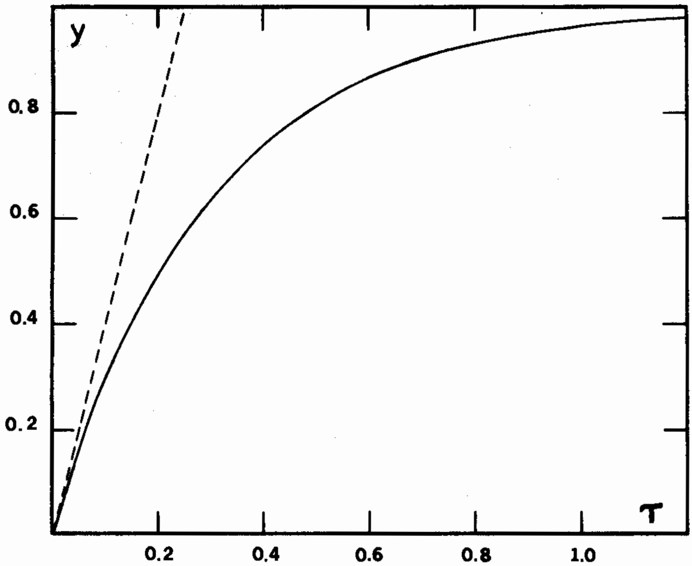

Fig. 2. The mean square displacement $\sigma(t)$ (eq. (2.15)) for a particle diffusing on a disc with a completely reflecting perimeter. The axes are in the dimensionless units $y = \sigma/a^2$ and $\tau = Dt/a^2$. The dashed line represents the asymptotic infinite plane result.

This has the following consequences for field ion microscopy: that marked deviations of $\sigma(t)$ occur from the infinite plane result. For O on the W(110) plane at $T = 1100$ K, the deviation is 10% for times $t \simeq 10^{-7}$ s for a typical plane of diameter 30 Å. Ir on the W(211) plane, at room temperature, yields a 10% error after $t \simeq 10^3$ s or a 2.5% error at $t \simeq 10^2$ s.

On the other hand for completely absorbing boundaries we find

$$\sigma(t) = 8a^2\left\{\frac{1}{16} - \sum_{n=1}^{\infty} \frac{2}{\beta_{0n}^4} \exp\left(-D\beta_{0n}^2 t/a^2\right)\right\}, \tag{2.17}$$

where

$$J_0(\beta_{0n}) = 0, \tag{2.18}$$

which has the same initial behavior,

$$\lim_{t\to 0} \sigma(t) = 0,$$

$$\lim_{t\to 0} \frac{\partial\sigma(t)}{\partial t} = \lim_{t\to 0} 4D \sum_{n=1}^{\infty} \frac{4}{\beta_{0n}^2} \exp\left(-D\beta_{0n}^2 t/a^2\right) = 4D,$$

as that for the reflecting boundaries. The full behavior is plotted in fig. 3.

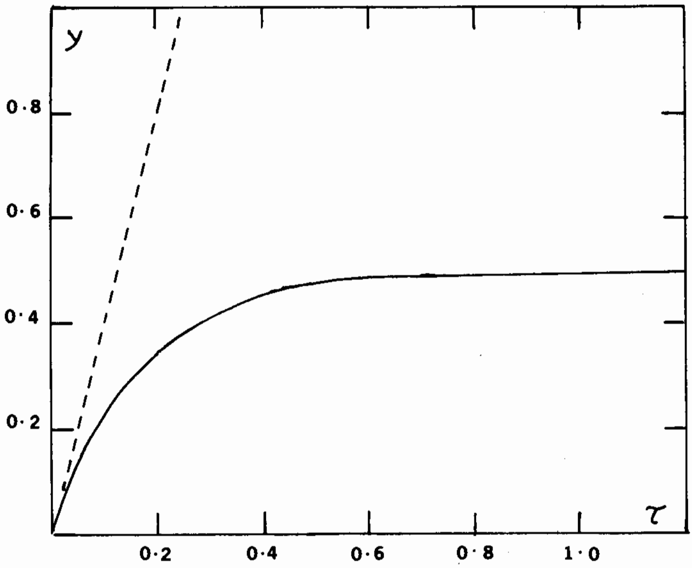

Fig. 3. The mean square displacement $\sigma(t)$ (eq. (2.17)) for a particle on a disc with an absorbing boundary. The dashed line corresponds to the asymptotic infinite plane result.

3. Discussion

Mössbauer measurements of an atom diffusing on a surface should exhibit a broadening. The broadening is dependent on the size of the surface, and on the boundary conditions in a characteristic way. In principle, one should be able to determine the diffusion coefficient D, the average radius of the surface a, as well as the nature of the boundary κ. These quantities may then be compared with the diffusion coefficients obtained from field ion microscopy techniques.

We also propose that Mössbauer measurements be performed on single simple metal surfaces that have islands or terraces [11]. Such experiments would be difficult to perform. The present state of the art Mössbauer measurements can be performed on single surfaces with areas of 10^{-4} m^2, with only milli-monolayers of Co coverage. However, the data collection time is of the order of half a day [12], and the data analysis must take into account the finite beam width. At helium temperatures, we expect that only the unbroadened natural line will be observed since the diffusion on surfaces usually involves a considerable activation energy [1]. As the temperature is increased towards room temperature, the spectrum will change its shape. The spectrum will then be composed of an un-broadened line of reduced strength superimposed on a broad background. Even though there is a distribution in the geometries and the sizes of the islands or terraces, it can be argued that the Mössbauer spectrum can be used to provide an estimate of the average inverse area of the size of the islands. Thus, if the Mössbauer technique that we have outlined is successful, the technique could be applied to the problem of surface characterization.

Acknowledgements

The authors would like to thank Marten den Boer and R.W. Hoffmann for stimulating discussions and helpful comments.

Appendix A

The Green function and Mössbauer spectrum for a particle diffusing on a disc

The conditional probability satisfying the diffusion equation

$$\frac{\partial}{\partial t} P(\boldsymbol{r}, \boldsymbol{r}_0|t) = D\,\nabla^2 P(\boldsymbol{r}, \boldsymbol{r}_0|t), \tag{A.0}$$

can be expressed uniquely in terms of a complete set of states

$$P(\boldsymbol{r}, \boldsymbol{r}_0|t) = \sum_{m=-\infty}^{\infty} \sum_{n=1}^{\infty} a_{mn}(t)\, J_m(\beta_{mn} r/a) \exp(-\mathrm{i} m\psi), \tag{A.1}$$

where β_{mn} are determined by the boundary condition

$$J_m(\beta_{mn}) + \kappa\beta_{mn} J_m'(\beta_{mn}) = 0. \tag{A.2}$$

On Laplace transforming (A.0) and using Bessels equation

$$J_m''(x) + \frac{1}{x} J_m'(x) + \left(1 - m^2/x^2\right) J_m(x) = 0, \tag{A.3}$$

and using the initial condition

$$P(\boldsymbol{r}, \boldsymbol{r}_0|0) = \delta(\boldsymbol{r} - \boldsymbol{r}_0), \tag{A.4}$$

we find

$$\sum_{mn} \left(\omega + D\beta_{mn}^2/a^2\right) \tilde{a}_{mn}(\omega)\, J_m(\beta_{mn} r/a) \exp(-\mathrm{i} m\psi)$$
$$= \frac{1}{r_0} \delta(r - r_0)\, \delta(\psi - \psi_0), \tag{A.5}$$

in which $\tilde{a}_{mn}(\omega)$ is the Laplace transform of $a_{mn}(t)$. The time dependence of $a_{mn}(t)$ is thus found to be

$$a_{mn}(t) = a_{mn}(0) \exp\left(-D\beta_{mn}^2 t/a^2\right). \tag{A.6}$$

The initial value $a_{mn}(0)$ is found from (A.5) by using the completeness relation (A.7) and then projecting out on the m, n eigenfunction of (A.0),

$$\frac{1}{r_0}\delta(r-r_0)\,\delta(\psi-\psi_0)$$
$$=\frac{1}{\pi a^2}\sum_{m=-\infty}^{\infty}\sum_{n=1}^{\infty}\frac{\exp[-\mathrm{i}m(\psi-\psi_0)]\,J_m(\beta_{mn}r/a)\,J_m(\beta_{mn}r_0/a)}{\left(1-m^2/\beta_{mn}^2\right)J_m^2(\beta_{mn})+J_m'^2(\beta_{mn})}. \tag{A.7}$$

The projection of eq. (A.5) on the eigenfunction is achieved by using Lommels second integral,

$$\int_0^x y\,J_m^2(\alpha y)\,\mathrm{d}y=\frac{x^2}{2}\left[J_m'^2(\alpha x)+\left(1-\frac{m^2}{\alpha^2x^2}\right)J_m^2(\alpha x)\right]. \tag{A.8}$$

The result for $a_{mn}(0)$ is then found to be

$$a_{mn}(0)=\frac{\kappa^2\beta_{mn}^2J_m(\beta_{mn}r_0/a)\exp(\mathrm{i}m\psi_0)}{\pi a^2\left[1+\kappa^2\left(\beta_{mn}^2-m^2\right)\right]J_m^2(\beta_{mn})}. \tag{A.9}$$

On using (A.9), (A.6) and (A.1) we find the result quoted in the text for $P(\boldsymbol{r}, \boldsymbol{r}_0|t)$ (eq. (2.10)). The result for $Q(\boldsymbol{r}, \boldsymbol{r}_0|t)$ follows directly from (2.10) by considering the net flux of particles on the boundary. Our results (2.10) and (2.11) satisfy the condition

$$\int\mathrm{d}\boldsymbol{r}\int\mathrm{d}\boldsymbol{r}_0\,p(\boldsymbol{r}_0)[P(\boldsymbol{r},\boldsymbol{r}_0|t)+Q(\boldsymbol{r},\boldsymbol{r}_0|t)]=\int\mathrm{d}\boldsymbol{r}_0\,p(\boldsymbol{r}_0),$$

for any arbitrary $p(\boldsymbol{r}_0)$. The Mössbauer spectrum is calculated from

$$\int\mathrm{d}\boldsymbol{r}\int\mathrm{d}\boldsymbol{r}_0[P(\boldsymbol{r},\boldsymbol{r}_0|t)+Q(\boldsymbol{r},\boldsymbol{r}_0|t)]\;p(\boldsymbol{r}_0)\exp\left(\mathrm{i}q_{\|}r\cos\psi-\mathrm{i}q_{\|}r_0\cos\psi_0\right). \tag{A.10}$$

We shall assume a uniform initial probability $p(r_0)=1/\pi a^2$. The contribution of $P(\boldsymbol{r}, \boldsymbol{r}_0|t)$ to the spectrum is found by rewriting (A.10) as

$$I_p(t)=\sum_{mn}\exp\left(-D\beta_{mn}^2t/a^2\right)$$
$$\times\int\frac{r\,\mathrm{d}r\,\mathrm{d}\psi J_m(\beta_{mn}r/a)\exp(-\mathrm{i}m\psi)\exp\left(\mathrm{i}q_{\|}r\cos\psi\right)\kappa\beta_{mn}}{\pi a^2J_m(\beta_{mn})\left[1+\kappa^2\left(\beta_{mn}^2-m^2\right)\right]^{1/2}}\times\{\ldots\}^*. \tag{A.11}$$

On using the generating function expansion

$$\exp\left(\mathrm{i}q_{\|}r\cos\psi\right)=\sum_{m=-\infty}^{\infty}J_m(q_{\|}r)\exp(\mathrm{i}m\psi), \tag{A.12}$$

and integrating over the area, we find

$$I_p(t)=\sum_{mn}\frac{4\exp(-D\beta_{mn}^2t/a^2)\,\beta_{mn}^2\left[J_m(q_\|a)+q_\|a\kappa J_m(q_\|a)\right]^2}{\left(q_\|^2a^2-\beta_{mn}^2\right)^2\left[1+\kappa^2(\beta_{mn}^2-m^2)\right]}. \tag{A.13}$$

The radial integrals involved are given by Lommels first integral

$$\int_0^x J_m(\alpha y)\,J_m(\beta y)\,y\,\mathrm{d}y=\frac{x}{\alpha^2-\beta^2}\left[\beta J_m(\alpha x)\,J_m'(\beta x)-\alpha J_m(\beta x)\,J_m'(\alpha x)\right]. \tag{A.14}$$

The Mössbauer spectrum from the particles bound to the perimeter $I_q(t)$ is found from

$$\begin{aligned}I_q(t)=&-\sum_{m=-\infty}^{\infty}\sum_{n=1}^{\infty}\left[1-\exp(-D\beta_{mn}^2t/a^2)\right]\\&\times\int\frac{r_0\,\mathrm{d}r_0\,\mathrm{d}\psi_0}{\pi a^2}\,\frac{J_m(\beta_{mn}r_0/a)}{J_m(\beta_{mn})}\,\frac{\kappa\beta_{mn}\exp(\mathrm{i}m\psi_0)\exp(-\mathrm{i}q_\|r_0\cos\psi_0)}{\left[1+\kappa^2(\beta_{mn}^2-m^2)\right]^{1/2}}\\&\times\int\frac{\mathrm{d}\psi}{\pi}\,\frac{J_m'(\beta_{mn})}{J_m(\beta_{mn})}\,\frac{\kappa\exp(-\mathrm{i}m\psi)\exp(\mathrm{i}q_\|a\cos\psi)}{\left[1+\kappa^2(\beta_{mn}^2-m^2)\right]^{1/2}},\end{aligned} \tag{A.15}$$

which yields

$$\begin{aligned}I_q(t)=&-\sum_{m=-\infty}^{\infty}\sum_{n=1}^{\infty}\left[1-\exp(-D\beta_{mn}^2t/a^2)\right]\\&\times\frac{4J_m(q_\|a)\left[J_m(q_\|a)+\kappa q_\|aJ_m'(q_\|a)\right]}{\left(q_\|^2a^2-\beta_{mn}^2\right)\left[1+\kappa^2(\beta_{mn}^2-m^2)\right]}.\end{aligned} \tag{A.16}$$

Combining (A.13) and (A.16), multiplying by $\frac{1}{2}\exp(-\frac{1}{2}\Gamma|t|)$ and Fourier transforming yields (2.12).

Appendix B

The mean square displacement of a particle diffusing on a disc with mixed boundary conditions

$$\sigma(t)=\int\mathrm{d}\boldsymbol{r}\int\mathrm{d}\boldsymbol{r}_0\,p(\boldsymbol{r}_0)\left[P(\boldsymbol{r},\boldsymbol{r}_0|t)+Q(\boldsymbol{r},\boldsymbol{r}_0|t)\right](\boldsymbol{r}-\boldsymbol{r}_0)^2. \tag{B.0}$$

We shall use the uniform initial probability $p(\boldsymbol{r}_0)=1/(\pi a^2)$. Separating the P and Q contributions of $\sigma(t)$, such as

$$\sigma(t)=\sigma_p(t)+\sigma_Q(t),$$

the contribution $\sigma_p(t)$ is evaluated first by integrating over the angles

$$\sigma_p(t) = \frac{4}{a^2} \sum_{m=-\infty}^{\infty} \int_0^a r\, \mathrm{d}r \int_0^a r_0\, \mathrm{d}r_0 \left[\left(r^2 + r_0^2 \right) \delta_{m,0} - r r_0 \left(\delta_{m,1} + \delta_{m,-1} \right) \right]$$
$$\times \sum_{n=1}^{\infty} \frac{\kappa^2 \beta_{mn}^2 J_m(\beta_{mn} r/a)\, J_m(\beta_{mn} r_0/a)}{\left[1 + \kappa^2 \left(\beta_{mn}^2 - m^2 \right) \right] J_m^2(\beta_{mn})} \exp\left[-D\beta_{mn}^2 t/a^2 \right]. \qquad \text{(B.1)}$$

The radial integrals are evaluated by using the relation

$$\int_0^x r^n J_m(\lambda r)\, \mathrm{d}r$$
$$= \frac{r^n}{\lambda} J_{m+1}(\lambda r) \bigg|_0^x + \frac{(m+1-n)}{\lambda} \int_0^x r^{n-1} J_{m+1}(\lambda r)\, \mathrm{d}r. \qquad \text{(B.2)}$$

Thus we obtain

$$\sigma_p(t) = 8a^2 \left\{ \sum_{n=1}^{\infty} \frac{\kappa^2 \left[\beta_{0n} J_1(\beta_{0n}) - 2J_2(\beta_{0n}) \right] J_1(\beta_{0n})}{\beta_{0n} \left(1 + \kappa^2 \beta_{0n}^2 \right) J_n^2(\beta_{0n})} \right.$$
$$\times \exp\left(-D\beta_{0n}^2 t/a^2 \right)$$
$$\left. - \sum_{n=1}^{\infty} \frac{\kappa^2 J_2^2(\beta_{1n})}{\left[1 + \kappa^2 \left(\beta_{1n}^2 - 1 \right) \right] J_1^2(\beta_{1n})} \exp\left(-D\beta_{1n}^2 t/a^2 \right) \right\}. \qquad \text{(B.3)}$$

Similarly,

$$\sigma_q(t) = \frac{4}{a^2} \sum_{m=-\infty}^{\infty} \int_0^a \mathrm{d}r_0 r_0 \left[\left(a^2 + r_0^2 \right) \delta_{m,0} - a r_0 \left(\delta_{m,1} + \delta_{m,-1} \right) \right]$$
$$\times \sum_{n=1}^{\infty} \frac{\kappa J_m(\beta_{mn} r_0/a)}{J_m(\beta_{mn})} \frac{1 - \exp\left(-D\beta_{mn}^2 t/a^2 \right)}{1 + \kappa^2 \left(\beta_{mn}^2 - m^2 \right)} \qquad \text{(B.4)}$$

which on integrating becomes

$$\sigma_q(t) = 8a^2 \left\{ \sum_{n=1}^{\infty} \frac{\kappa \left[\beta_{0n} J_1(\beta_{0n}) - J_2(\beta_{0n}) \right]}{J_0(\beta_{0n})\, \beta_{0n}^2 \left(1 + \kappa^2 \beta_{0n}^2 \right)} \left[1 - \exp\left(-D\beta_{0n}^2 t/a^2 \right) \right] \right.$$
$$\left. - \sum_{n=1}^{\infty} \frac{\kappa J_2(\beta_{1n})}{J_1(\beta_{1n})\, \beta_{1n} \left[1 + \kappa^2 \left(\beta_{1n}^2 - 1 \right) \right]} \left[1 - \exp\left(-D\beta_{1n}^2 t/a^2 \right) \right] \right\}. \qquad \text{(B.5)}$$

Using the recursion relations

$$J_{m+1}(z) = \frac{m}{z} J_m(z) - J_m'(z),$$

and

$$J'_{m+1}(z)=\frac{(m+1)}{z}J'_m(z)+\left(1-\frac{m(m+1)}{z^2}\right)J_m(z), \tag{B.6}$$

we find

$$\sigma_p(t)=8a^2\left\{\sum_{n=1}^{\infty}\frac{\beta_{0n}^2(1+2\kappa)-4}{\beta_{0n}^4(1+\kappa^2\beta_{0n}^2)}\exp(-D\beta_{0n}^2t/a^2)\right.$$
$$\left.-\sum_{n=1}^{\infty}\frac{(\kappa+1)^2}{\beta_{1n}^2[1+\kappa^2(\beta_{1n}^2-1)]}\exp(-D\beta_{1n}^2t/a^2)\right\}, \tag{B.7}$$

and

$$\sigma_q(t)=8a^2\left\{\sum_{n=1}^{\infty}\frac{\beta_{0n}^2(1+\kappa)-2}{\beta_{0n}^4(1+\kappa^2\beta_{0n}^2)}[1-\exp(-D\beta_{0n}^2t/a^2)]\right.$$
$$\left.-\sum_{n=1}^{\infty}\frac{(\kappa+1)}{\beta_{1n}^2[1+\kappa^2(\beta_{1n}^2-1)]}[1-\exp(-D\beta_{1n}^2t/a^2)]\right\}, \tag{B.8}$$

which combine to yield eq. (2.14) of the text.

Appendix C

Some useful properties of the zeros of Bessel functions

This appendix is concerned with an extension of Rayleigh's formulae for the zeros of $J_m(x)$,

$$J_m(\alpha_{mn})=0. \tag{C.0}$$

Rayleigh [12] has shown

$$\sum_{n=1}^{\infty}\frac{1}{\alpha_{mn}^2}=\frac{1}{4(m+1)}, \tag{C.1}$$

$$\sum_{n=1}^{\infty}\frac{1}{\alpha_{mn}^4}=\frac{1}{16(m+1)^2(m+2)}, \tag{C.2}$$

etc. We shall derive similar formulae, for the zeros of $J'_m(x)$,

$$J'_m(\beta_{mn})=0. \tag{C.3}$$

Consider the expansion [13]

$$J'_m(z)=\frac{(z/2)^{m-1}}{2(m-1)}\prod_{u=1}^{\infty}\left(1-\frac{z^2}{\beta_{mn}^2}\right). \tag{C.4}$$

Forming the logarithmic derivative, we find

$$J_m''(z) = J_m'(z) \sum_{n=1}^{\infty} \left(\frac{2z}{\beta_{mn}^2 - z^2} + \frac{1-m}{z} \right). \tag{C.5}$$

On substituting Bessels equation in (C.5) and substituting $z = m$, we find our first result,

$$1 = \sum_{n=1}^{\infty} \frac{2m}{\beta_{mn}^2 - m^2}. \tag{C.6}$$

Our second result follows from inserting the series expansion for $J_m'(z)$ in both sides of (C.5). Collecting like powers of z, produces the equality

$$\frac{m+2}{4m(m+1)} = \sum_{n=1}^{\infty} \frac{1}{\beta_{mn}^2}, \tag{C.7}$$

and similar equalities for

$$\sum_{n=1}^{\infty} \frac{1}{\beta_{mn}^{2r}}.$$

References

[1] For recent reviews, see G. Ehrlich and K. Stolt, Ann. Rev. Phys. Chem. 31 (1980) 603; J. Vacuum Sci. Technol. 17 (1980) 9.
[2] G. Ehrlich, Phys. Today (June 1981) p. 44.
[3] E.W. Müller, Ergeb. Exakt. Naturw. 27 (1953) 290;
E.W. Müller and T.T. Tsong, Field Ion Microscopy (Elsevier, New York, 1968).
[4] K.S. Singwi and A. Sjölander, Phys. Rev. 120 (1960) 1093.
[5] J.H. Jensen, Physik Kondens. Materie 13 (1971) 273.
[6] H. Keller and P.G. Debrunner, Phys. Rev. Letters 45 (1980) 68.
[7] F. Parak, E.N. Frolov, R.L. Mössbauer and V.I. Goldanskii, J. Mol. Biol. 145 (1981) 825.
[8] T.G. Dewey and G.G. Hammes, Biophys. J. 32 (1980) 1023.
[9] C. Kittel, Quantum Theory of Solids (Wiley, New York, 1963).
[10] K. Ito, Stochastic Differentials, Appl. Math. Opt. 1 (1975) 374.
[11] A.M. Glass, P.F. Liao, J.G. Bergman and D.H. Olson, Optics Letters 5 (1980) 368.
[12] R.W. Hoffman, private communication.
[13] G. Watson, Theory of Bessel Functions, 2nd ed. (Cambridge University Press, 1962).